Anomalous spin-wave behavior in the magnetic alloy Fe_xCr_{1-x}

S. M. Shapiro and C. R. Fincher, Jr.*
Brookhaven National Laboratory, Upton, New York, 11973

A. C. Palumbo
Department of Physics, University of Rochester, Rochester, New York 14627

R. D. Parks
Department of Physics, Polytechnic Institute of New York, Brooklyn, New York 11201

(Received 15 July 1981)

Neutron scattering methods are employed to study the temperature and magnetic field dependence of the spin dynamics in the alloy Fe_xCr_{1-x} for $x=0.34$, 0.28, 0.26, 0.24, and 0.22. For $x=0.34$ and 0.28, the system orders ferromagnetically and exhibits well-defined spin waves throughout the ferromagnetic phase. For $x \leq 0.26$, ferromagnetism is also present but at low temperatures a spin-glass-like phase exists. For these concentrations the spin-wave excitations are observed within the ferromagnetic phase but as the temperature is lowered towards the spin-glass regime the spin-wave frequency decreases. At low temperatures, within the spin-glass regime, no well-defined excitations are present, but an intense quasielastic peak is observed. Application of a magnetic field causes a reemergence of the spin-wave excitations.

I. INTRODUCTION

A spin-glass can be defined as a magnetic system, which is characterized by a random freezing of the moments in such a way that no long-range magnetic order is present.[1] The most intensely studied systems are the metallic alloys such as $Au_{1-x}Fe_x$ and $Cu_{1-x}Mn_x$. An important feature of this definition is that it implies a well-defined transition temperature, T_f, where the spins are frozen into a random orientation. T_f is evidenced most strongly by a sharp cusp in the low-field magnetic susceptibility measurements[2] and a splitting of the lines in the Mössbauer spectra.[3] Other properties which would be sensitive to cooperative effects occurring in a phase transition such as the specific heat,[2] show no anomaly at T_f. Likewise, the electrical resistivity varies smoothly through T_f.[4] Thus, there is an intense debate whether a well-defined phase transition to a spin-glass state exists.

In the theories treating spin-glasses, many of the thermodynamic techniques developed for the study of phase transitions in equilibria systems have been applied to spin-glasses.[5] Edwards and Anderson (EA) defined an order parameter for a spin-glass[6] and Sherrington and Kirkpatrick (SK) calculated a phase diagram.[7] In the former, the specific heat also exhibited an anomaly and in the latter there were problems such as negative entropy at low temperatures. Recent calculations and computer studies have increased the debate amongst the theorists about the existence of a well-defined phase transition in spin-glasses with common dimensionality.[8]

The other key feature of the definition is that no spontaneous magnetization is present. This has led to a picture of a spin-glass as comprised of clusters of limited number of spins with some degree of order within the cluster. These clusters form at high temperatures. As T is lowered, the clusters interact with one another until T_f, when they lock into a configuration where the total magnetic moment is zero.

Recently, it has been shown that as one varies the concentration of the magnetic impurities, an interesting sequence of transitions can occur.[9] At high temperatures, the system is in a paramagnetic (PM) state and as the temperature is lowered to the Curie temperature T_C, the system enters a ferromagnetic (FM) state where long-range magnetic order exists. As the temperature is reduced further, the system enters a spin-glass (SG) state at $T=T_f$. We shall refer to these systems as spin-glasses although the nature of the low-temperature phase is not completely clear.

Such a sequence of phase transitions was actually predicted by SK.[7] They presented a solvable model of a spin-glass where the spins are coupled by infinite ranged random exchange interactions described by a Gaussian probability density:

$$P(J_{ij}) = \frac{1}{\sqrt{2\pi J^2}} \exp[(J_{ij}-J_0)/2J^2] \quad . \tag{1}$$

In Eq. (1), J_0 is the mean value of the exchange and the distribution width J is a measure of the spin-glass interaction. For $|J_0/J| >> 1$ long-range order exists. For J_0 comparable to J there will be some spins ex-

periencing a positive J_{ij} and others a negative J_{ij} which leads to the competing ferro- and antiferromagnetic interactions necessary for the spin-glass state. The phase diagram calculated by SK shows that for $\tilde{J}_0/\tilde{J}$ ($\tilde{J}_0 = NJ$ and $\tilde{J} = \sqrt{NJ}$, where N is the number of spins) between 1.0 and 1.25, the sequence, PM to FM to SG phases, occurs on decreasing temperature.

This sequence of phases was experimentally demonstrated in the $(PdFe)_{1-x}Mn_x$ system by low field dc susceptibility measurements.[9] The magnetic susceptibility exhibits a flat region within the ferromagnetic regime due to demagnetizing effects and then a drop at both T_c and T_f. Several other systems exhibit similar behavior: $(Fe_{1-x})_3Al_x$,[10] the ionic solid $Eu_xSr_{1-x}S$,[11] the amorphous alloy $(Fe_xMn_{1-x})_{75}P_{16}B_6Al_3$,[12] and the alloy Fe_xCr_{1-x}[13] which is the subject of the present investigation.

$Eu_xSr_{1-x}S$ is particularly interesting because the interactions are understood. They are the near neighbor exchange which is positive and the next-nearest-neighbor exchange which is negative and has a value about half the near neighbor exchange. Thus the problem reduces in part to a statistical one connected very closely with percolation theories. In fact, Binder *et al.* used series expansion and Monte Carlo methods to study the low-temperature state and have been successful in reproducing portions of the measured phase diagram.[14]

$Eu_xSr_{1-x}S$ is also experimentally very interesting in that Eu^{2+} is an S-state ion and possesses a large free-ion magnetic moment: $\mu = 7.0\mu_B$. Thus, the magnetic Bragg scattering is sufficiently strong to be observable in a neutron scattering experiment. Maletta *et al.* have performed extensive neutron-diffraction experiments on $Eu_xSr_{1-x}S$ for a wide range of x.[11,15] For $0.5 < x < 0.6$ they observe an increase in the Bragg scattering at T_c which is due to the onset of long-range ferromagnetic magnetic order. This intensity increases with decreasing temperature until T_f where the intensity decreases again. It is not clear yet whether the long-range order completely disappears or some order remains at $T = 0$. This is the only spin-glass system where the zero field magnetization has been measured.

The susceptibility of Fe_xCr_{1-x} alloy exhibits the behavior typical of a reentrant spin-glass.[13] Figure 1(a) shows the susceptibility measured in a sphere of $Fe_{0.34}Cr_{0.66}$. Below $T_c \simeq 330$ K, the susceptibility is constant due to demagnetization effects all the way down to the lowest temperature. This is the behavior typical of a ferromagnetic. Figure 1(b) shows the behavior for a $Fe_{0.22}Cr_{0.78}$ sample. The susceptibility increases as T decreases, levels off near T_c, and then decreases at lower temperatures, the behavior typical of a reentrant spin-glass.

Bulk magnetization and diffuse neutron scattering studies show that for x between 0.20 and 0.30, the

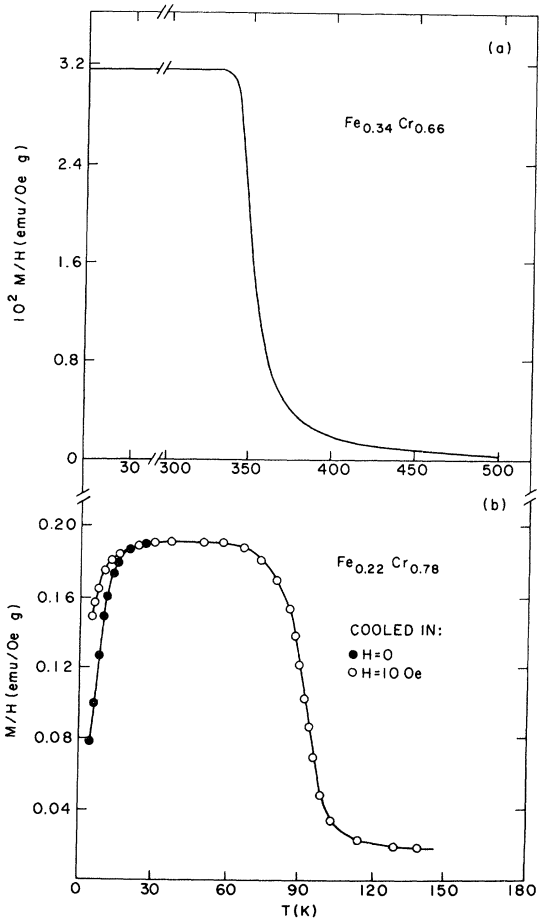

FIG. 1. (a) dc magnetization of $Fe_{0.34}Cr_{0.66}$ sphere measured in 100 Oe. (b) dc magnetization of $Fe_{0.22}Cr_{0.78}$ sphere; (○): cooled in zero field measured in 10 Oe; (●): cooled in 10 Oe measured in 10 Oe.

chromium atom contains no moment and the magnetization is less than $0.5\mu_B$.[16,17] This makes observation of the long-range order difficult to observe in a neutron-diffraction study. On the other hand, the spin-wave energies are in a convenient energy and temperature range to allow study by inelastic neutron scattering techniques. Since we can enter the SG state directly from a FM state, our goal is to study the evolution of the spin dynamics on entering the SG phase. Thus we can build upon our understanding of spin waves in a FM to gain insight into the spin dynamics of a SG. This approach, we believe, provides more information than studying directly the PM-SG transition. We shall study the temperature, momentum, and field dependence of the spin waves. The most striking feature of our results is the anomalous temperature renormalization of the spin-wave energies for those alloys which show the anomalous low-temperature behavior. The spin-wave

energies increase below T_c, reach a maximum as T is decreased and decrease again as the low-temperature spin-glass state is approached.[18]

II. SAMPLES AND EXPERIMENTAL DETAILS

A. Samples

The studies were performed on polycrystalline Fe_xCr_{1-x} alloys with $x=0.34$, 0.28, 0.26, 0.24, and 0.22. The samples were prepared from 99.99% starting material, arc melted, annealed for 4 d at 1100 °C and water quenched. They were then reannealed at 1000 °C for another day to remove strains. The samples were either button-shaped or spherical. A 1-cm-diameter, 2-mm-thick piece was cut from the $x=0.34$ sample and a microprobe analysis performed. The result gave a concentration of $x=0.334(6)$ with negligible variation over the sample.

On all samples studied, a powder diffraction pattern was taken from $Q=0.1$ to 4.5 Å^{-1} to check for sample homogeneity. The results from $x=0.34$ and 0.22 at room temperature are shown in Fig. 2. These were performed on a triple-axis machine set for zero energy transfer. Only the bcc powder peaks were present. Rotation of the sample with the scattering arm set for the (110) reflection revealed large variations in intensity indicating the existence of small

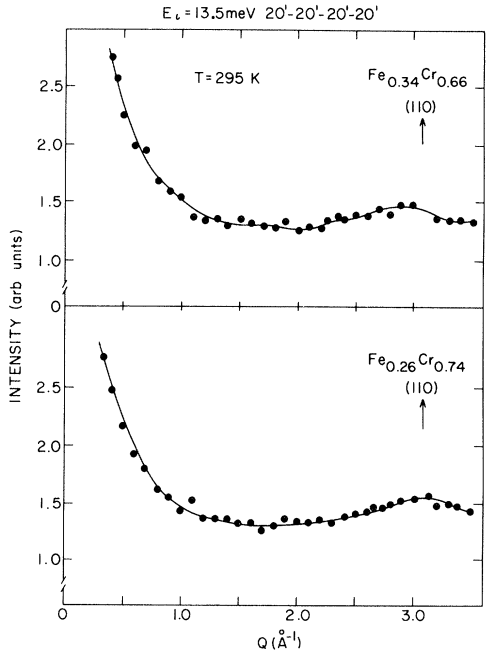

FIG. 2. Diffraction pattern of $Fe_{0.34}Cr_{0.66}$ and $Fe_{0.26}Cr_{0.74}$ polycrystalline sample measured at room temperature. Arrow indicates location of (110) Bragg peak. The Q resolution is less than the size of the symbols.

crystallites with preferred orientation. This, however, will not affect the inelastic measurements made at small momentum transfers.

The major feature of the diffraction pattern is the large amount of diffuse scattering for the small-Q values and the broad hump about the (110) Bragg peaks. This type of scattering has been studied extensively for Fe_xCr_{1-x} (Refs. 17 and 19) and other magnetic alloys,[20] and is due to the chemical short-range nonrandomness of the alloy. Diffraction patterns were performed at temperatures down to 10 K with negligible change except for the very-small-Q region. This nuclear clustering most likely plays an important role in the magnetic properties of Fe_xCr_{1-x}, and in the magnetic behavior of spin-glasses in general. There have been some limited studies on the effect of annealing on the magnetic phase diagram of $Au_{1-x}Fe_x$,[21] but the role of nulcear clustering in spin-glasses remains largely unexplored.

From their study of diffuse scattering, Aldred *et al.*[17] find that for the iron-rich alloys, there is a long-range disturbance in the moment at the iron atoms which gives way to a more local disturbance as the chromium concentration increases. At around $x=0.20$, where the ferromagnetism disappears, large polarization "clouds" are expected. These "clouds" do not show any strong temperature dependence and their role in the magnetic ordering and the spin dyanmics is uncertain. Since, in the present experiment, we are probing very long wavelength excitations ($\lambda \equiv 2\pi/Q \sim 50$–$200$ Å), the effects of short-range clusters are probably not important.

B. Experimental details

The neutron scattering measurements were performed at Brookhaven National Laboratory's High Flux Beam Reactor. A pyrolytic graphite (PG) monochromator [(002) reflection] provided an incident energy (E_i) of either 13.5, 5.0, or 3.8 meV. A PG (002) analyzer was used. The collimations were 20-10-10-20, 20-20-20-20, and 20-20-20-40 for $E_i=13.5$, 5.0, and 3.8 meV, respectively, where the numbers are the horizontal divergencies from reactor to monochromator, to sample, to analyzer, and to detector. The full width at half maximum (FWHM) energy resolution for zero energy transfer is 0.30, 0.08, and 0.06 meV for $E_i=13.5$, 5.0, and 3.8 meV, respectively. For 13.5 meV, a PG filter was used to eliminate the higher-order contamination of the beam, while for the lower energies, a cooled beryllium filter eliminated the higher order. Since polycrystalline samples were used, all inelastic measurements were performed near the forward direction, the (0,0,0) Bragg peak. Constant-Q scans were performed with fixed E_i for Q values ranging from $Q=0.05$ Å^{-1} to 0.2 Å^{-1}. Since the first zone boun-

dary, $\frac{1}{2}(110)$, occurs at $Q=1.5$ Å^{-1}, the measurements are limited to the first tenth of the Brillouin zone. Any line broadening due to powder averaging of the magnon dispersion is negligible at these small wave vectors and is ignored in our treatment.

Measurements of the critical scattering were performed down to $Q=0.03$ Å^{-1} with the anlayzer set for zero energy transfer. Because we are measuring at very small scattering angles, it is very important to carefully mask the sample in order to reduce the background. This background is very Q dependent due to contamination by the direct beam. As we shall see, an accurate determination of the background is one of the major problems in the analysis of our results.

All samples were mounted in a He-filled aluminum can and placed on the cold finger of a flow cryostat or a closed cycle Air Products Displex refrigerator. The temperature range covered was between 4.5 and 350 K with regulation better than 0.1 K. For the magnetic field studies, a split coil superconducting magnet was used with the field direction perpendicular to the horizontal scattering plane.

III. SCATTERING CROSS SECTION

As a starting point in understanding our experiment, we shall assume the cross section for inelastic scattering from a FM is applicable. The cross section can be written in several different forms.[22] We shall follow the formalism used by Dietrich *et al.*[23] for a Heisenberg FM. The scattering cross section can be written

$$\frac{d^2\sigma}{d\Omega\, d\omega}=A\frac{k_f}{k_i}\frac{\hbar\omega/kT}{1-\exp(-\hbar\omega/kT)}\chi_0^{-1} \times\left[\tfrac{2}{3}\chi_Q^t F^t(Q,\omega)+\tfrac{1}{3}\chi_Q^l F^l(Q,\omega)\right] . \quad (2)$$

The coefficient A contains some trivial constants including the magnetic form factor $f(\vec{Q})$ which is nearly unity since we are measuring at such small momentum transfers. k_f and k_i are the initial and final values of the neutron wave vectors. χ_0 is the susceptibility of an isolated ion and $\chi_0 \sim T^{-1}$. The superscripts t and l refer to the transverse and longitudinal response. Since we are dealing with spin waves mainly below T_c, we concern ourselves only with χ_Q^t which behaves as $\chi_Q^t \sim Q^{-2}$ for the small-Q limit. The cross section then reduces to

$$\frac{d^2\sigma}{d\Omega\, d\omega}=A'\frac{k_f}{k_i}\frac{\hbar\omega/kT}{1-\exp(\hbar\omega/kT)}\frac{F(Q,\omega)}{Q^2} \quad (3)$$

with $A' \sim T$.

$F(Q,\omega)$ is the normalized spectral weight function and contains the dynamics of the spin interactions. The problem arising in choosing the form of $F(Q,\omega)$ has been previously discussed.[23] The three forms generally used are (1) a double Lorentzian; (2) a damped harmonic oscillator; and (3) a form suggested by Halperin and Hohenberg.[24] When a sharp peak is present, all three forms reduce to the same function. When the width of the peak becomes comparable to its position, all three forms adequately describe the data, but the resulting parameters may be very different. There is no theoretical justification for choosing one of the three forms but a double-peaked Lorentzian is usually used. We shall follow that custom here. Thus

$$F(Q,\omega)=\frac{1}{2\pi}\left[\frac{\Gamma}{(\omega-\omega_Q)^2+\Gamma^2}+\frac{\Gamma}{(\omega+\omega_Q)^2+\Gamma^2}\right], \quad (4)$$

where $\hbar\Gamma$ is the half-width at half maximum (HWHM) and $\hbar\omega_Q$ represents the energy of the excitation. Since measurements are restricted to small Q, the dispersion law for spin waves in a FM takes the form:

$$\hbar\omega_Q=\Delta+DQ^2 , \quad (5)$$

where D is the magnetic stiffness constant and Δ is the gap due to anisotropy effects, either intrinsic, or a Zeeman splitting due to an applied field

$$\Delta=\Delta_0+g\mu_B H . \quad (6)$$

The dispersion is assumed to be isotropic so that $\hbar\omega_Q$ depends only on the magnitude of Q.

To analyze the data, we have to consider the instrumental resolution. An analytical form of the resolution function of a triple-axis spectrometer exists and has been sufficiently tested.[25] We convolute the resolution function with the form of the cross section given in Eq. (3) and compare the results with the measured intensity. A generalized least-squares routine is used to find the values of the parameters in the cross section which minimize the weighted mean square deviation between the calculated and measured intensities. The adjustable parameters are A', D, and Γ. A constant energy independent background is subtracted from all spectra. Its value was determined from the counting rate at large energy transfers.

IV. RESULTS AND COMPARISON WITH SPIN-WAVE THEORY

A. Elastic scattering

The temperature variation of the intensities measured at $Q=0.04$ Å^{-1} for $x=0.34$, 0.26, and 0.22 is shown in Fig. 3. These data were taken on a triple-axis spectrometer set for zero energy transfer. The incident energy was $E_i=13.7$ meV for $x=0.34$ and

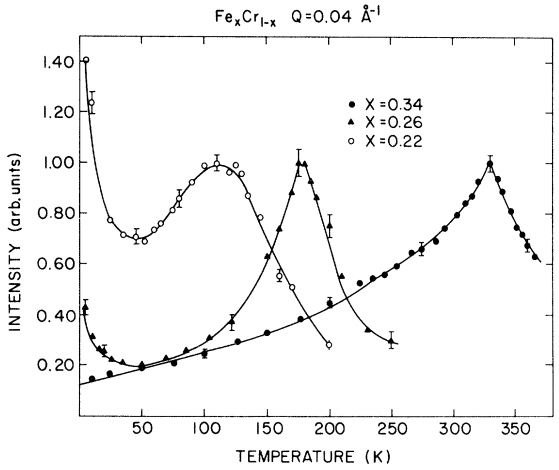

FIG. 3. Elastic scattering measured at $Q=0.04$ Å^{-1} for $\Delta E=0$ for Fe_xCr_{1-x}, $x=0.22$, 0.26, and 0.34. The intensities have been normalized to the same value at the transition temperatures.

0.22, and $E_i=5.0$ meV for $x=0.26$. The intensities are normalized to be the same value at the Curie temperature. The Q value indicated is that measured in the scattering plane. However, since the vertical resolution is comparable to this value, the nominal Q is larger than the value indicated. A more appropriate experiment to measure intensities at these small momenta would be the use of a small angle scattering facility employing an area detector. This has been performed for Fe_xCr_{1-x} by Burke *et al.*[26] and Shapiro *et al.*[27] and the present results are similar to theirs. A peak is clearly observable at the Curie temperature for each alloy and T_c is tabulated in Table I. For $x=0.34$, the intensity decreases monotonically below T_c which is typical behavior of a ferromagnet. The quantity being measured is the integral over energy of Eq. (3) since Q is small and ω_Q is much less than

TABLE I. Transition temperatures and spin-wave parameters for Fe_xCr_{1-x}.

x	T_c (K)	D (meV Å^2)	Δ_0 (meV)
0.34	330 ±2	58.3 ±2[a]	0.01 ±0.01
0.28	209 ±3	30.0 ±2[a]	0.01 ±0.01
0.26	178 ±3	19.7 ±1[b]	0.03 ±0.01
0.24	125 ±5	11.5 ±4[b]	. . .
0.22	110 ±5	. . .	. . .

[a]Measured at $T=50$ K.
[b]Measured at $T=75$ K.

the instrumental resolution. Thus

$$\frac{d\sigma}{d\Omega}=\int\frac{d\sigma}{d\Omega\,d\omega}\sim\frac{\chi_q}{\chi_0}\sim T\ . \tag{7}$$

This is why at lower temperatures for $x=0.34$, the intensity varies linearly with T. For $x=0.26$ and 0.22, a very different behavior is observed. The intensity also peaks at T_c, decreases below T_c, but at lower temperatures it begins to increase again. As x decreases, the realtive increase at low temperatures becomes more pronounced and the peak at T_c is more rounded.

From these results we construct the phase diagram given in Fig. 4. The small x, Cr-rich, regime exhibits interesting antiferromagnetic behavior and that part of the phase diagram has been taken from the literature.[28] T_c is linear in x and extrapolates to 0 K at $x=0.16$ in agreement with some other studies.[17,26] Our data do not exhibit any sharp peak or any other feature that defines a sharp transition from the ferromagnetic to a spin-glass-like state. The hatched region denotes the range of T and x studied where anomalous magnetic behavior is observed as evidenced by the upswing at low temperatures shown in Fig. 3 and the temperature dependence of the spin-wave energies discussed below. We shall follow convention and use the term "spin-glass" in discussing the low-temperature state, but we emphasize that the precise nature of this state is unclear.

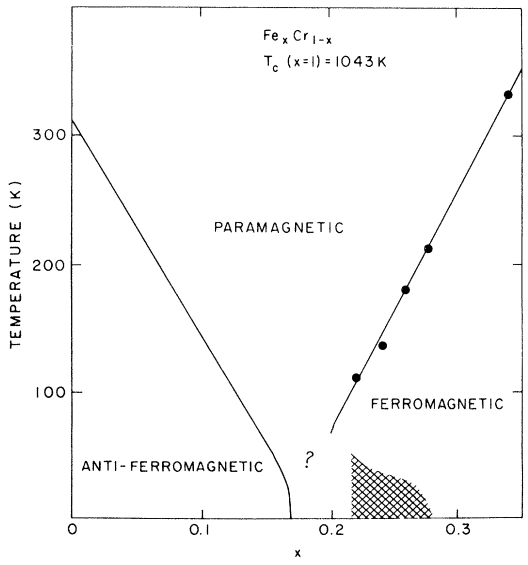

FIG. 4. Temperature-concentration phase diagram as deduced from our data given in Table I. The hatched area denotes the region of anomalous magnetic behavior. The small concentration region of the phase diagram is taken from Ref. 28. The question mark denotes the uncertainty about the magnetic state.

The temperature dependence of the intensity in Fig. 3 is very similar to that observed in other systems exhibiting the degradation of ferromagnetism with decreasing temperature such as $Eu_xSr_{1-x}S$ [15] and $(PdFe)_{1-x}Mn_x$,[9,29] and the amorphous alloys $(Fe_xMn_{1-x})_{75}P_{16}B_6Al_3$,[12,30] TbFe,[31] and YFe_2.[31]

The Q dependence of the small angle scattering was not explored in detail in the present experiment but the results of Burke *et al.*[26] on Fe_xCr_{1-x} show a striking similarity to the results obtained on other reentrant systems listed above.[15,29] For those x's where a FM phase exists, the intensity at $T > T_c$ follows the normal Ornstein-Zernike behavior expected for a FM

$$\chi_Q^{-1} \sim (\kappa^2 + Q^2) \ , \tag{8}$$

where κ is the inverse of the correlation. κ decreases as T approaches T_c and remains zero in the FM phase. When a SG phase occurs below the FM phase, there are large deviations from OZ behavior, and κ remains small.

B. Inelastic results

We shall present the main features of the temperature dependence of the inelastic scattering by discussing the results for $x = 0.34$ and $x = 0.26$. Figure 5 shows the observed spectra for $Fe_{0.34}Cr_{0.66}$ at several temperatures below T_c. These spectra were taken with $E_i = 13.5$ meV and $Q = 0.075$ Å^{-1}. A three-peaked structure is seen with peaks at $\Delta E = \pm\hbar\omega_Q$ and $\Delta E = 0$. The inelastic peaks are due to spin waves and the $\Delta E = 0$ peak is the elastic background. It is temperature independent and is composed of nuclear incoherent scattering, scattering from the cryostat and, most importantly, contamination from the direct beam because the scattering angle is so small ($2\theta = 1.7°$). This elastic background has a FWHM equal to the instrumental resolution and is subtracted from all spectra to yield the reduced spectra of Fig. 6.

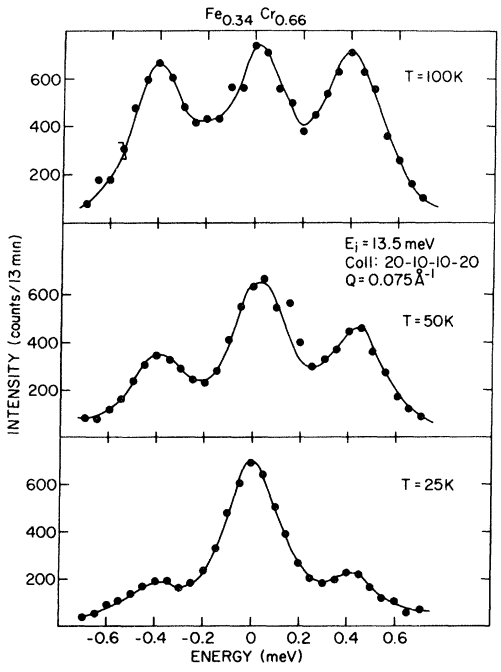

FIG. 5. Experimentally observed spectra for $Fe_{0.34}Cr_{0.66}$ at several temperatures measured at $Q = 0.075$ Å^{-1}.

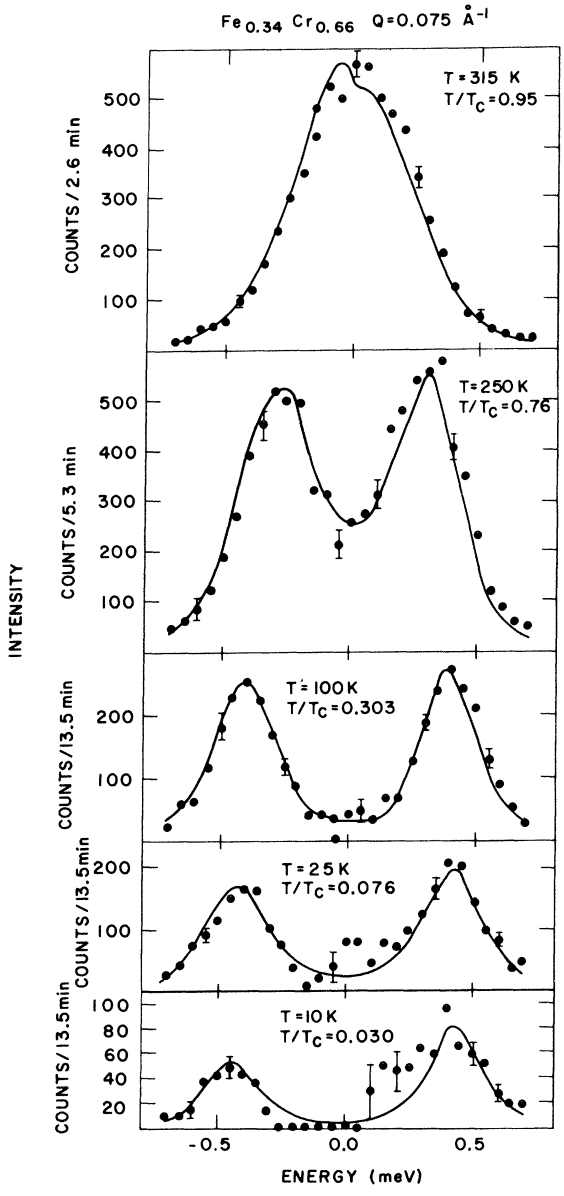

FIG. 6. Temperature dependence spectra of $Fe_{0.34}Cr_{0.66}$ ($T_c = 330$ K) after subtraction of elastic background. Solid lines are a fit to the data as described in the text.

It is clearly seen that the spin-wave energy increases as T decreases below T_c and becomes constant with temprature at sufficiently low temperatures.

The temperature dependence of the spectra for $x=0.26$ is very different. Figure 7 shows the observed spectra at several temperatures below $T_c=180$ K. These were obtained with an incident energy of $E_i=4.5$ meV and at $Q=0.075$ Å^{-1}. At $T=75$ K, the spectrum shows a three-peaked structure with spin waves at $\Delta E=\hbar\omega_q$ and an elastic peak at $\Delta E=0$. When excitations are well defined, the elastic peak is temperature independent. We assume that this is the background and subtract it from all spectra. The reduced spectra are shown in Fig. 8. The temperature dependence is remarkably different from the $x=0.34$ sample in that at low temperatures, the spin-wave frequency *decreases* as T decreases.

The corrected spectra are fit to the cross section of Eq. (3) using Eq. (4) folded with the resolution function. The solid lines of Figs. 6 and 8 are a result of such fits to the data. For $x=0.26$, and below $T=20$ K, no well-defined excitations are observed and for these spectra we let $\hbar\omega_Q=0$ in Eq. (4). The spectra are then described by a single Lorentzian centered about $\Delta E=0$ with HWHM of Γ. A reasonable fit can also be obtained if a small, but finite, value of D is chosen with a large value of Γ. Since the maximum of the observed signal is at $E=0$, we choose to describe the spectra by a single broadened

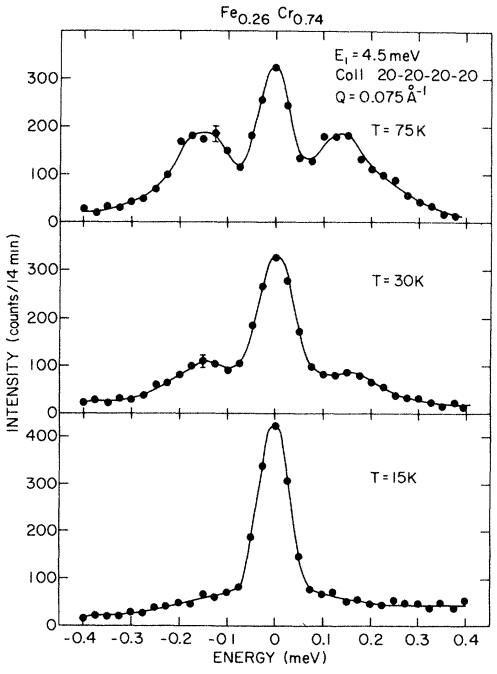

FIG. 7. Experimentally observed spectra for $Fe_{0.26}Cr_{0.74}$ at several temperatures measured at $Q=0.075$ Å^{-1}.

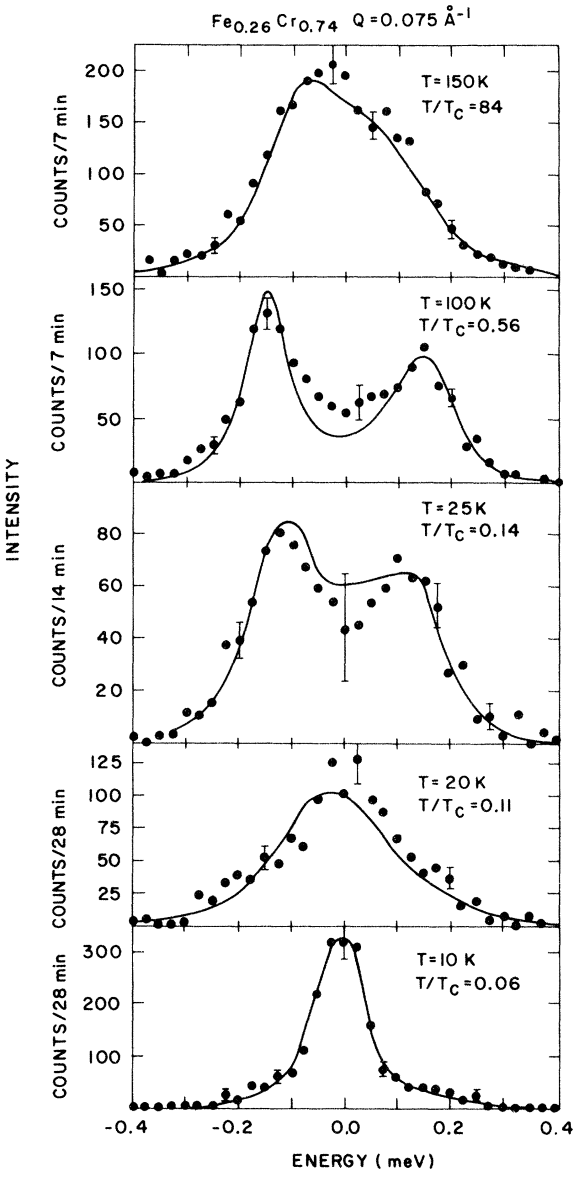

FIG. 8. Temperature dependent spectra of $Fe_{0.26}Cr_{0.74}$ ($T_c=178$ K) after subtraction of elastic background. Solid lines are a fit to the data as described in the text.

Lorentzian. The spectra are initially broader than the resolution width and as T decreases further, the linewidth narrows and becomes resolution limited at the lowest temperatures.

The parameters obtained from the fit are shown in Figs. 9–11. Figure 9(a) shows the temperature dependence of the magnetic stiffness measured at $Q=0.075$ Å^{-1} for $x=0.34$. It exhibits the behavior typical of a ferromagnet: an increase below T_c and eventual saturation at low temperatures. In Fig. 9(b) the behavior of D for $x=0.26$ is shown. Near T_c, it

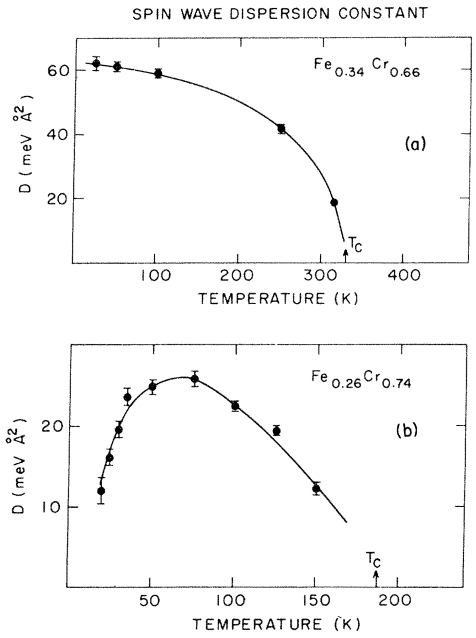

FIG. 9. Temperature dependence of magnetic stiffness D for Fe_xCr_{1-x} as determined from the spectra in Fig. 6 and Fig. 8. (a) $x=0.34$, (b) $x=0.26$.

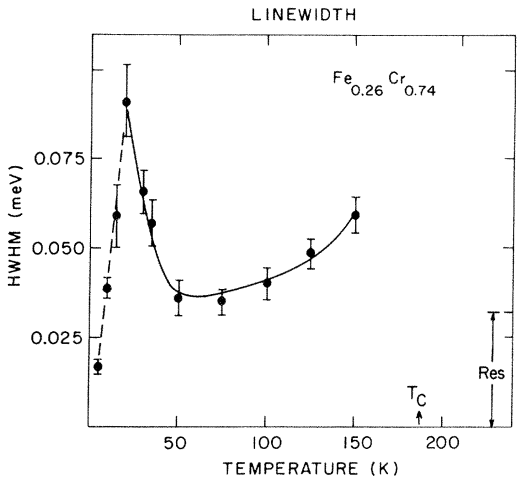

FIG. 10. The observed linewidth Γ for $Fe_{0.26}Cr_{0.74}$. For $T>25$ K (solid line), well-defined spin waves exist and represent the HWHM of the excitation. For $T<25$ K (dashed lines), Γ represents the HWHM of the line centered about $\Delta E=0$, i.e., D was set to 0.

behaves similarly to that of a ferromagnet, but below about 60 K, the stiffness begins to decrease. This temperature corresponds closely to the temperature, where the small angle critical scattering begins to increase.

The other parameters obtained from a fit to the data also show anomalous behavior for $x=0.26$. The temperature dependence of the linewidth Γ is shown in Fig. 10. For $x=0.34$ (not shown) the linewidth was always less than instrumental except near T_c. For $x=0.26$ above 60 K, the temperature dependence is typical of a FM. Below this temperature Γ increases until 20 K when no propagating excitations are observed and we begin to describe our spectra with a single Lorentzian centered at $E=0$ with linewidth Γ. The decrease for $T<20$ K reflects the narrowing of the quasielastic linewidth.

The normalization parameter divided by the temperature, $\chi_Q/(\chi_0 T)$, is shown in Fig. 11. For a FM, it is constant according to Eq. (3) and such is the case for $x=0.34$. However, for $x=0.26$, there is an increase at the lower temperatures. This is additional evidence that conventional spin-wave theory breaks down for $x=0.26$.

Spin waves were also observed for $x=0.28$ and behaved very similarly to the $x=0.34$ sample. For $x=0.22$, the energy of the spin waves was too low such that we were unable to observe any well-defined excitations. Only broad quasielastic scattering was observed.

We now examine in more detail the wave vector (Q) and magnetic field (H) dependence of the spin dynamics in the ferromagnetic, spin-glass, and paramagnetic regimes.

Whenever well-defined spin waves are observed, they follow a quadratic Q dependence given by Eq. (5). A plot of spin-wave energy versus Q^2 is shown in Fig. 12(a) for $Fe_{0.26}Cr_{0.74}$ at $T=75$ K. A gap of

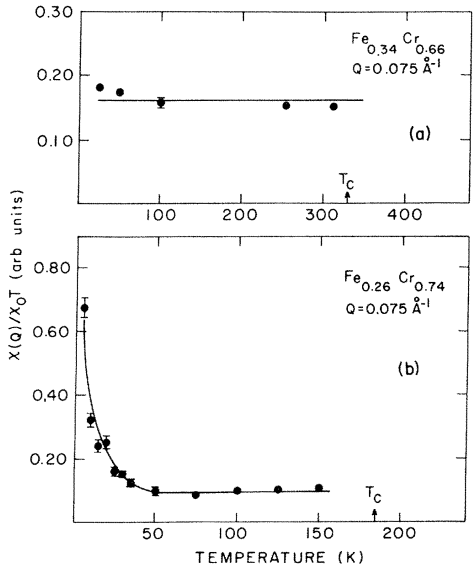

FIG. 11. $\chi(Q)/\chi_0 T$ vs T for Fe_xCr_{1-x} as deduced from our inelastic spectra spin-wave theory predicts a straight line as observed for $Fe_{0.34}Cr_{0.66}$. (a) $x=0.34$, (b) $x=0.26$.

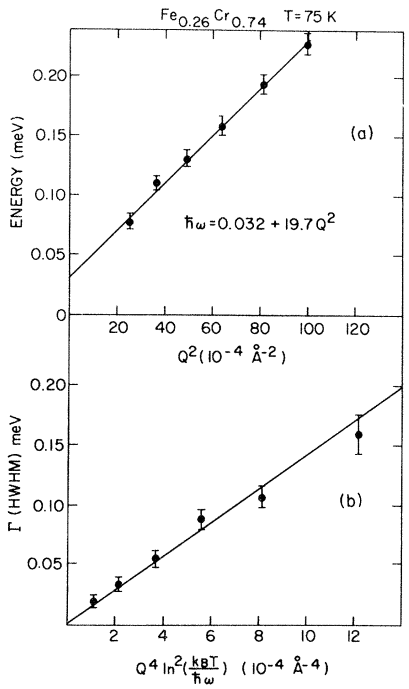

FIG. 12. (a) Measurements of spin-wave energy as a function of Q^2 for $Fe_{0.26}Cr_{0.74}$ at $T=75$ K, in the ferromagnetic regime. (b) Spin-wave linewidth measured at $T=75$ K. The straight line indicates that Γ follows the prediction based upon magnon-magnon interaction.

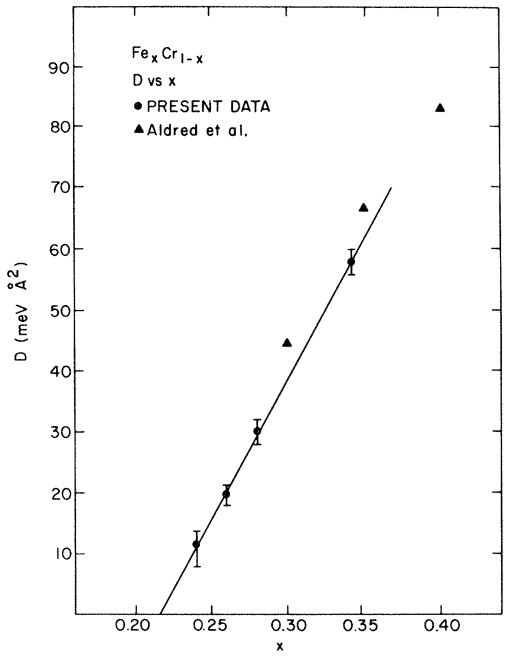

FIG. 13. The concentration dependence of the spin-wave stiffness for Fe_xCr_{1-x} measured within the ferromagnetic phase. The triangles are values obtained from the temperature dependence of the magnetization (Ref. 16).

$\Delta_0 = 0.03 \pm 0.01$ meV is measured. Similar curves were obtained for other x's and Table I gives for the value of D and Δ_0 obtained. Figure 13 is a plot of D vs x near 50 K. D varies linearly with x and extrapolates to 0 at $x=0.217$. For comparison, the values of D obtained by Aldred[16] from low-temperature magnetization measurements are also given. In the overlapping regime, the agreement is reasonably good.

The linewidth also increases with Q consistent with the predictions from spin-wave theory. The expected Q dependence of the linewidth comes from a Green's function calculation of the magnon-magnon interactions in a cubic lattice.[32] In the Q regime accessible to neutron scattering

$$\Gamma(Q) \sim T^2Q^4\ln^2\left(\frac{k_BT}{\hbar\omega_Q}\right) . \tag{9}$$

In Fig. 12(b) we plot Γ measured at $T=75$ K versus $Q^4\ln^2(k_BT/\hbar\omega_Q)$ for $x=0.26$. It is clear that the data follow the theoretical predictions.

For $x=0.26$ and temperatures less than 60 K, the spin-wave energies decrease and for $T<20$ K no propagating features were observed (see Fig. 8). The difficulty in analyzing the data is the subtraction of the elastic background which, in many cases, is a significant fraction of the observed signal. The background can be determined from measurements in the ferromagnetic regime as discussed above and by measurements of the spectra in large fields (see below). Figure 14 shows the Q dependence of the spectra measured for zero field at $T=15$ K, within the hatched region of Fig. 4. The background has already been subtracted. The observed, uncorrected spectrum is shown in the top portion of Fig. 15. The solid lines in Fig. 14 are the results of fits to the data using Eqs. (3) and (4) with $\hbar\omega_Q=0$. The values of Γ are indicated in the figure and the insert is a plot of Γ vs Q. Γ increases rapidly with Q but we cannot give the precise behavior due to the large uncertainties as a result of the subtraction, especially for the larger Q values. The important result is that a diffusive behavior exists, i.e., Γ increases with Q.

At low temperatures, we applied a magnetic field to $Fe_{0.26}Cr_{0.74}$. The field dependence of the scattering for $Q=0.03$ Å^{-1} measured at $T=5.0$ K is shown in Fig. 16(a). Figure 16(a) shows that the scattering decreases with increasing field and becomes field independent for $H>6$ kOe. A decrease of the small angle scattering with increasing field was previously observed by Burke *et al.*[26] The effect of the field on the temperature dependence of the small angle scattering is shown in Fig. 16(b). The solid points are a remeasure of the T dependence shown in Fig. 3, but with better resolution: $\delta E(\text{HWHM}) \simeq 0.03$ meV. At 10 kOe, the scattering is temperature in-

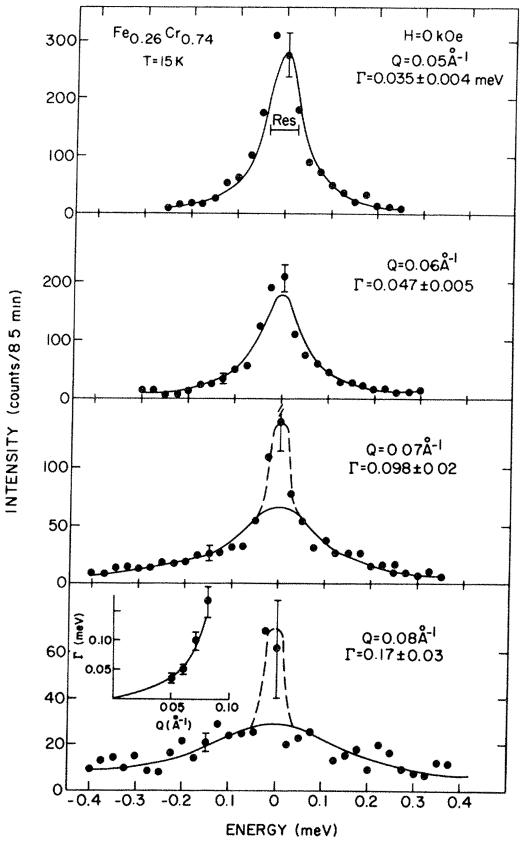

FIG. 14. The Q dependence of the spectra of $Fe_{0.26}Cr_{0.74}$ measured within the SG phase. The elastic background determined from high field data of Fig. 16 has been subtracted. The solid line is a fit to a Lorentzian and the Q dependence of the linewidth is shown as an inset.

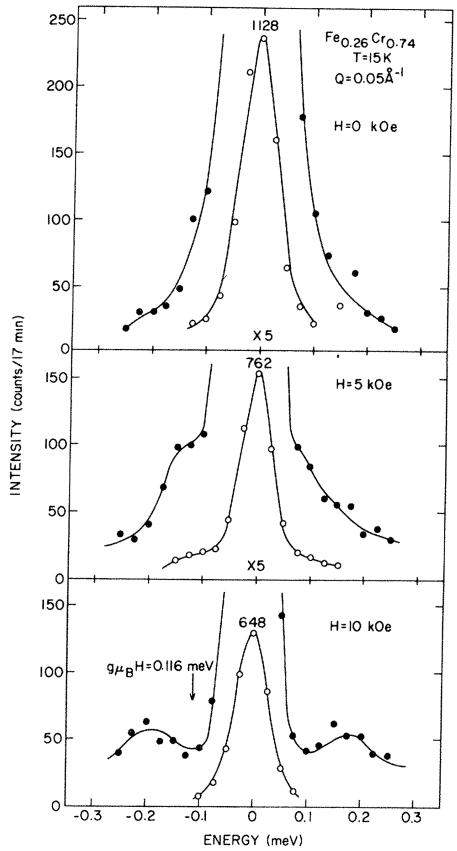

FIG. 15. Magnetic field dependence of quasielastic scattering measured at $T=10$ kOe at $Q=0.05$ Å^{-1}. For $H=10$ kOe, the Zeeman term $g\mu_B H=0.116$ meV with $g=2$ is indicated.

dependent and the observed level is the background. This is immediately understood from Eq. (5) which shows that a magnetic field causes a gap to appear in the spin-wave dispersion equal to the Zeeman splitting: $\Delta E=g\mu_B H=0.0116$ meV/kOe for $g=2$. For an applied field of 10 kOe, $\Delta E=0.116$ meV which is much larger than the instrumental energy resolution. Thus under application of a field, the intensity becomes inelastic and is pushed out beyond the resolution window of the instrument.

The spectra under applied field at $Q=0.05$ Å^{-1} is shown in Fig. 15. No subtractions have been performed. At $H=0$ kOe, an intense peak centered at $\Delta E=0$ is present. As the field increases, the intensity of the center part decreases and shoulders begin to develop for 5.0 kOe. For 10 kOe, the central part has decreased even further and well-defined peaks appear at finite energies. These peaks are at an energy larger than that expected from just the Zeeman term. From the Q dependence of the spectrum, we obtain a value of $D=21.3\pm3$ meV Å^2 which is similar to the maximum value of D obtained within the FM regime.

The solid line in Fig. 15 for $H=10$ kOe is the fit to the data with the above D and a Gaussian at $\Delta E=0$ with the instrumental width. This Gaussian is temperature independent, but strongly Q dependent and is the best estimate of the elastic background.

Measurements were performed in the paramagnetic regime above T_c on the $Fe_{0.26}Cr_{0.74}$ sample. If we define the critical region as the temperature range where critical scattering is observed, then from Fig. 3 we see that the critical region increases as T_c approaches the SG regime. For example, for $x=0.22$, significant critical scattering is observed over a reduced temperature range $\epsilon\equiv(T-T_c)/T_c=0.8$ whereas for $x=0.26$, the range is reduced to $\epsilon=0.4$. Figure 17(a) shows inelastic scans for different Q

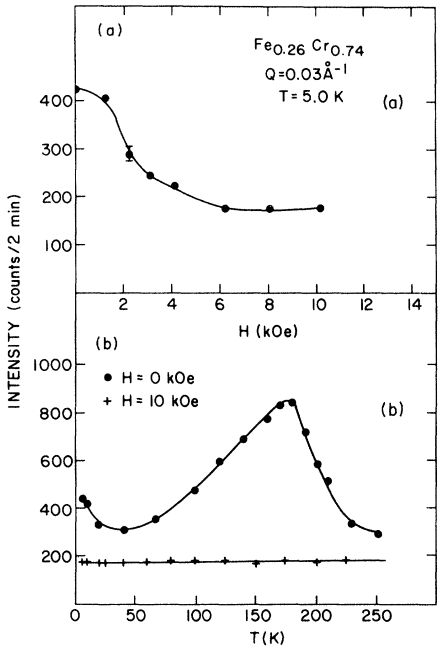

FIG. 16. (a) Field dependence of the elastic scattered intensity for $Fe_{0.26}Cr_{0.74}$ measured at $T=5.0$ K. (b) Temperature dependence of the scattered intensity measured at $Q=0.03$ Å^{-1} with $H=0$ kOe and 10 kOe. Both sets of data can be interpreted as creation of inelastic scattering whose energy becomes larger than the resolution.

values measured at $T=225$ K ($\epsilon=0.25$) for the $x=0.26$ sample. The elastic background has been subtracted. This was determined by the high-field measurements shown in Fig. 17(b). Under application of a field, the spectra exhibit a three-peaked structure and the elastic portion is assumed to be the background. The $H=0$ kOe spectra exhibit a quasielastic peak which is broader than the instrumental resolution and increases with increasing Q. This is characteristic of spin diffusion in ferromagnets observed at small wave vectors for $T \geq T_c$. Only a limited number of Q values were measured and the linewidth follows the power law $\Gamma \sim q^z$ with $z=2.2 \pm 0.3$. From the integrated intensity, we can obtain an estimate of the inverse correlation length $\kappa=0.08 \pm 0.04$ Å^{-1}. Thus, our measurements are within the hydrodynamic regime where the linewidth is expected to follow a q^2 power law, which is consistent with the data. The important result is that for a large range of reduced temperatures above T_c, the spin dynamics behave as expected for a typical ferromagnet.

An applied field causes a dramatic change of the spectra as shown in Fig. 17(b). The top portion shows the spectrum before (dashed line) and after (full line) subtraction of $\Delta E=0$ background. Well-defined excitations are observed which are larger than the expected Zeeman splitting. From the Q

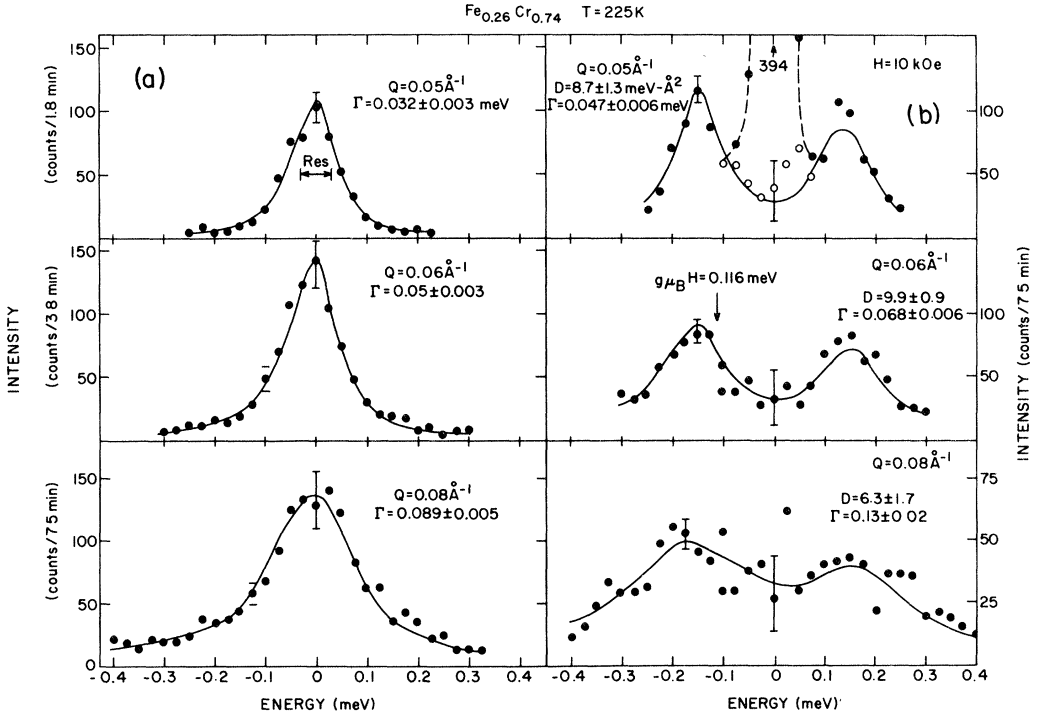

FIG. 17. Q dependence of quasielastic scattering in $Fe_{0.25}Cr_{0.74}$ measured at 225 K, greater than T_c. (a) zero field; (b) field of $H=10$ kOe. The solid lines are fits to the data and the parameters obtained are shown.

dependence, we obtain an average value for $D = 8.2 \pm 1.3$ meV Å^2. Propagating excitations seem to be present under an applied field.

V. DISCUSSION

The major result of this study is the breakdown of spin-wave theory at low temperatures for Fe_xCr_{1-x} with $x \leq 0.26$. Within the ferromagnetic regime, for temperatures $T/T_c > 0.2$, Fe_xCr_{1-x} seems to behave like a conventional ferromagnetic as evidenced by the magnetic stiffness, the susceptibility, and the Q dependence of the linewidth. A more detailed study of the critical properties may reveal deviations from expected 3D Heisenberg behavior, but at this stage, it appears that the dilution of Fe with Cr has the effect of reducing the energy scale of the system by sharply reducing T_c.

For $T/T_c < 0.2$, a different magnetic state is being approached which has many of the characteristics of a spin-glass state. The excitation spectra (Fig. 14) look similar to what has been observed in the more typical spin-glass systems such as Fe_xAu_{1-x},[33] and $Cu_{1-x}Mn_x$.[34] In these spin-glass systems, a broadened quasielastic line is present, but an additional resolution-limited elastic peak is also present. As the temperature decreases, the elastic intensity increases.[33,34] We observe in Fe_xCr_{1-x} only one quasielastic peak centered around $\Delta E = 0$ whose width narrows as the temperature decreases. The elastic peak may be present in our data, but with the resolution used we were unable to decompose the spectra into two peaks centered around $\Delta E = 0$. The existence of the unresolved elastic peak may be the reason for the upswing at low temperatures of the normalized susceptibility shown in Fig. 11. The cross section given in Eq. (3) does not explicitly allow for an elastic component. Recent measurements on $Eu_xSr_{1-x}S$ have shown similar features in the SG phase.[35] Because the energy scale and the temperature are so low, the inelastic scattering could be interpreted either as a broad propagating spin wave, or quasielastic scattering with a Q dependent linewidth. In addition, a resolution limited elastic peak was also observed.

There have been theoretical predictions about the dynamics in spin-glass although the predictions vary.[36] Some argue that propagating spin waves exist at $T = 0$ in a Heisenberg spin-glass but for $T \neq 0$ they are overdamped.[37] Krey uses numerical methods to study the dynamics of $Eu_xSr_{1-x}S$ and finds magnon peaks in the spin-glass phase, though they are quite broad.[38] Halperin and Saslow presented a theory in the hydrodynamic limit and proposed that if spin waves exist, they should possess a linear dispersion relation.[39] However, they also pointed out that if a nonzero magnetization remained, there would be a branch with a quadratic Q dependence. Our results in the SG phase are more consistent with diffusive behavior but it may be necessary to go to smaller wave vectors to observe a propagating excitation. This requires more resolution than presently available.

The major property we were unable to study is the long-range magnetic order since the moment is too small. In $Eu_xSr_{1-x}S$, the long-range order has been probed[11,15] and we shall assume that the zero-field magnetization behaves in a similar manner: an increase at T_c and a decrease at lower temperatures. Supporting evidence for this assumption is that the low-field susceptibility [Fig. 1(b)] behaves similarly with temperature, and the temperature dependence of the small angle scattering shown in Fig. 3 is similar for the two systems.

Insight into the low-temperature behavior of the spin waves may be obtained by comparing the results at lower temperatures with the known behavior of a ferromagnet upon approaching T_c. Because of thermal fluctuations, the system breaks up into correlated regions and the magnetization decreases from its saturation value. The resulting decrease in molecular field reduces the restoring force for the spin waves and critical slowing down with a decrease in D occurs. Now, as the SG regime is approached upon decreasing the temperature, clusters of correlated spins freeze out such that the long-range order is decreased. The molecular field must also decrease which causes a decrease in the stiffness. The important unknown quantity is the driving mechanism for the decrease in the magnetization at low temperatures. A possible candidate is the random dipolar forces present in the alloy. The energy associated with dipolar forces is small, on the order of a few degrees Kelvin, so at first thought they would not be strong enough to effect changes at 50 K. On the other hand, since the ferromagnetic sites are random and highly diluted, one is led to a visualization of the spin-glass-like state as being composed of ferromagnetic clusters. If dipolar effects between the clusters are involved then the relevant energies associated with such effects are proportional to the number of spins in a cluster, and the energies are scaled up to higher values.

It is interesting to note that the extrapolation of D vs x in Fig. 13 to $D = 0$ yields a critical value of x which is close to the percolation threshold calculated for a diluted bcc lattice: $x_c = 0.243$.[40] This linear dependence of D vs x has also been predicted from Monte Carlo techniques applied to the percolation problem.[40] The identification with the percolation problem is based, in part, on the fact that in this concentration regime chromium does not possess a moment.[17] The degradation of long-range magnetic order in Fe_xCr_{1-x} with decreasing temperature may be

viewed as a property of the dilute ferromagnet which does not require the presence of competing ferro- and antiferromagnetic interactions customarily used in the description of spin-glasses. The explanation of the complete phase diagram shown in Fig. 4 will be more complicated than the theories describing the phase diagrams in randomly mixed magnets.[41] The system has to be viewed as having one magnetic species with a moment varying with x. The phase diagram then divides itself into regions of competing interactions separated by a region where dilute ferromagnetism dominates.

There is strong evidence to suggest that the SG state existing at temperatures blow the FM state differs from the SG state obtained upon cooling directly from the PM state. The small angle scattering measurements on Fe_xCr_{1-x} (Refs. 26 and 27) and Eu_xSr_{1-x} (Ref. 15) show that when the SG state is preceded by a FM phase, the low-temperature spectra deviate strongly from the Q-dependent behavior predicted by Eq. (8). If forced to follow Eq. (8) over a limited Q regime, the resultant κ is nearly zero and the susceptibility diverges at $Q=0$. On the other hand, if no FM state occurs before the SG phase, and in conventional spin-glasses, the susceptibility determined from Eq. (8) does not diverge, i.e., κ remains finite. This behavior can be explained on the FM side of the phase diagram if the FM state never completely disappears. This leads to a picture where the infinite cluster breaks up into smaller disoriented clusters, but a long-ranged network still remains. The moment would then be reduced, while some long-range order remaining implies that a finite value of the stiffness remains at low temperatures. A similar picture has been proposed[42] to explain the small angle scattering results on Fe_xCr_{1-x}. This most likely is what is occurring. This description also connects very closely to the percolation problem. In fact, Cowley *et al.*[43] proposed similar arguments to describe the decrease in magnetization at low temperatures observed near the percolation limit in $KMn_xZn_{1-x}F_3$, a 3D antiferromagnet.

Another description of the low-temperature state of the reentrant spin-glasses may be that described recently by Aharony and Pytte.[44] They show that in systems with random fields or isotropic dipolar interactions, the magnetization is zero in zero field at any temperature and the susceptibility is infinite below a transition temperature and remains infinite at all temperatures below the transition temperature. The susceptibility should follow a $1/Q^2$ behavior, indicative of a power-law decay of the spin correlations. This implies that κ of Eq. (8) is zero. What destroys the long-range order are the spin fluctuations. The time scale of these fluctuations is slow and they may be the very long wavelength spin waves present in the spin-glass. A problem arises in that the state described by Aharony and Pytte occurs directly from the PM state, whereas the state we are describing evolves from a FM state. Clearly, detailed studies of the critical scattering, preferably on single crystals, are needed to confirm the magnetic nature of the low-temperature state.

On application of a magnetic field, we recover the spin waves as shown in Fig. 16. Evidently, we are destroying the spin-glass state by forcing the alignment of the spins. It is interesting to note that the spin-wave stiffness D measured in the SG state under an applid field is the same value as the maximum achieved within the FM regime with zero field. This suggests that 10 kOe aligns all the spins that were aligned within the FM phase. There may be other spins in finite size clusters that were never aligned and fields of more than 10 kOe are necessary to align these.

The results above T_c are interesting. Firstly, it appears that the critical region is unusually large. This may be a result of a change in the effective dimensionality which occurs in systems where random interactions play an important role. For lower dimensional systems, critical scattering is always observed over a large temperature range. Another explanation is that the prefactor describing the temperature dependence of the inverse correlation length is enhanced because of competing energy scales in the problem. Such an enhancement of the critical region has been observed in the 3D singlet ground-state system Pr_3Tl where there is the competition between crystal field and exchange energies.[45] In the Fe_xCr_{1-x} case, the competing energies may be the strong short-range exchange energy and the weaker energy coupling the clusters. Secondly, under an applied field of 10 kOe, we observe a propagating excitation as shown in Fig. 17(b). The existence of propagting excitations at small momenta above T_c is an unusual occurrence. On one hand, it seems surprising that a field of 10 kOe, equivalent to only 1.3 K, would be enough to overcome the thermal effects at 225 K. On the other hand, if the susceptibility is enhanced by the presence of ferromagnetic clusters, a small field can induce a macroscopic moment which results in propagating spin waves.

In summary, we have performed inelastic neutron scattering experiments on the Fe_xCr_{1-x} magnetic alloy. These measurements reveal interesting dynamical effects which have not been observed before. Spin-wave excitations are observed at small Q in the ferromagnetic regime and an anomalous decrease in spin-wave stiffness occurs as we approach the low-temperature spin-glass-like regime. The field and momenta dependencies of these excitations have also been studied. Since the spin-wave theory for ferromagnets is well understood, we expect that by probing the deviations from spin-wave theory, we shall obtain a more complete understanding of the dynamical effects in spin-glasses.

ACKNOWLEGMENTS

We thank G. Aeppli, R. J. Birgeneau, J. L. Black, H. Maletta, A. P. Murani, and G. F. Reiter for many helpful discussions and suggestions. We are also indebted to R. J. Birgeneau and G. Shirane for a critical reading of the manuscript. The work at Brookhaven was supported by the Division of Basic Energy Sciences, U.S. Department of Energy, under Contract No. DE-AC02-76CH00016. The work at Polytechnic Institute of New York and the University of Rochester was supported by the U.S. Office of Naval Research.

---

*Present address: Department of Physics, University of Pennsylvania, Philadelphia, Penn. 19174.

[1]J. A. Mydosh, J. Magn. Magn. Mater. 7, 237 (1978).

[2]L. E. Wenger and P. H. Keeson, Phys. Rev. B 11, 3497 (1975).

[3]C. E. Violet and R. J. Borg, Phys. Rev. 149, 540 (1966); 162, 608 (1967).

[4]P. J. Ford and J. A. Mydosh, Phys. Rev. B 14, 2057 (1976).

[5]For a review of the various theoretical approaches, see A. Blandin, J. Phys. (Paris) 39, C6-1499 (1978).

[6]S. F. Edwards and P. W. Anderson, J. Phys. F 5, 965 (1975).

[7]D. Sherrington and S. Kirkpatrick, Phys. Rev. Lett. 35, 1792 (1975); S. Kirkpatrick and D. Sherrington, Phys. Rev. B 17, 4384 (1978).

[8]A. J. Bray, M. A. Moore, and P. Reed, J. Magn. Magn. Mater. 15-18, 102 (1980).

[9]B. H. Verbeek, G. J. Nieuwenhuys, H. Stocker, and J. A. Mydosh, Phys. Rev. Lett. 40, 586 (1978).

[10]R. D. Shull, H. Okamoto, and P. A. Beck, Solid State Commun. 20, 863 (1976).

[11]H. Maletta and P. Convert, Phys. Rev. Lett. 42, 108 (1979).

[12]Y. Yeshurun, M. B. Salamon, K. V. Rao, and H. S. Chen, Phys. Rev. Lett. 45, 1366 (1980).

[13]R. D. Shull and P. A. Beck, in *Magnetism and Magnetic Materials—1974,* edited by C. D. Graham, G. H. Lander, and J. J. Rhyne, AIP Conf. Proc. No. 24 (AIP, New York, 1975), p. 95.

[14]K. Binder, W. Kinzel, and D. Stauffer, Z. Phys. B 36, 161 (1979).

[15]H. Maletta and W. Felsch, Z. Phys. B 37, 55 (1980).

[16]A. T. Aldred, Phys. Rev. B 14, 219 (1976).

[17]A. T. Aldred, B. D. Rainford, J. S. Kouvel, and T. J. Hicks, Phys. Rev. B 14, 228 (1976).

[18]C. R. Fincher, Jr., S. M. Shapiro, A. C. Palumbo, and R. D. Parks, Phys. Rev. Lett. 45, 474 (1980).

[19]F. Kajzar, G. Parette, and B. Babic (unpublished).

[20]R. W. Medina and J. W. Cable, Phys. Rev. B 15, 1539 (1977).

[21]S. Crane and H. Clauss, Solid State Commun. 35, 461 (1980).

[22]W. Marshall and S. W. Lovesey, *Theory of Thermal Neutron Scattering* (Oxford, London, 1971).

[23]O. W. Dietrich, J. Als-Nielsen, and L. Passell, Phys. Rev. B 14, 4923 (1976).

[24]B. I. Halperin and P. C. Hohenberg, Phys. Rev. 177, 952 (1969).

[25]N. J. Chesser and J. D. Axe, Acta Crystallogr. Sect. A 29, 160 (1973).

[26]S. K. Burke, R. Cywinski, and B. D. Rainford, J. Appl. Crystallogr. 11, 644 (1978).

[27]S. M. Shapiro, C. R. Fincher, Jr., W. C. Koehler, and H. R. Child, J. Appl. Crystallogr. (in press).

[28]Y. Ishikawa, S. Hoshino, and Y. Endoh, J. Phys. Soc. Jpn. 22, 1221 (1967); B. Loegel, J. Phys. F 5, 497 (1975).

[29]S. M. Shapiro, G. Shirane, B. H. Verbeek, G. J. Nieuwenhuys, and J. A. Mydosh, Solid State Commun. 36, 167 (1980).

[30]G. Aeppli, S. M. Shapiro, R. J. Birgeneau, and H. S. Chen (unpublished).

[31]S. J. Pickart, J. J. Rhyne, and H. A. Alperin, Phys. Rev. Lett. 33, 424 (1974).

[32]A. B. Harris, Phys. Rev. 175, 674 (1968); 184, 606 (1969).

[33]A. P. Murani, *Neutron Inelastic Scattering, 1977* (International Atomic Energy Agency, Vienna, 1978), Vol. II, p. 213.

[34]A. P. Murani, J. Phys. (Paris) 39, C6-1517 (1978).

[35]H. Maletta, W. Zinn, H. Scheuer, and S. M. Shapiro, J. Appl. Phys. 52, 1735 (1981).

[36]L. R. Walker and R. E. Walstedt, Phys. Rev. B 22, 3816 (1980).

[37]D. L. Huber and W. Y. Ching, Phys. Rev. (in press).

[38]U. Krey, Z. Phys. B 38, 243 (1980).

[39]B. I. Halperin and W. M. Saslow, Phys. Rev. B 16, 2154 (1977).

[40]S. Kirkpatrick, Solid State Commun. 12, 1279 (1973).

[41]S. Fishman and A. Aharony, Phys. Rev. B 18, 3507 (1978); 19, 3776 (1978).

[42]B. D. Rainford, J. Magn. Magn. Mater. 14, 197 (1979).

[43]R. A. Cowley, G. Shirane, R. J. Birgeneau, E. C. Svensson, and H. J. Guggenheim, Phys. Rev. B 22, 4412 (1980).

[44]A. Aharony and E. Pytte, Phys. Rev. Lett. 45, 1583 (1980).

[45]J. Als-Nielsen, J. K. Kjems, W. J. L. Buyers, and R. J. Birgeneau, J. Phys. C 10, 2673 (1977).